JACC Vol. 15, No. 4
March 15, 1990:890–9

# Preload Dependence of Fiber Shortening Rate in Conscious Dogs With Left Ventricular Hypertrophy

ISRAEL MIRSKY, PhD, FACC, TERUHIKO AOYAGI, MD, VALERIE MARION CROCKER, MS, ALAN M. FUJII, MD

*Boston and Southborough, Massachusetts*

**Employing the new concept of systolic myocardial stiffness, this study addresses the questions of linearity of the end-systolic stress-strain relations in left ventricular hypertrophy and the preload dependence of fiber shortening rate. Pressure overload hypertrophy was induced in six puppies by banding the ascending aorta. Ultrasonic crystals were implanted for measurement of short axis and wall thickness in the six dogs with hypertrophy and in five control dogs. A pressure catheter was inserted through the apex for left ventricular pressure measurement. Load was altered by graded infusions of phenylephrine in the setting of beta-adrenergic blockade.**

**Linearity of the end-systolic stress-strain relations was observed in all cases, and preload-corrected shortening rate-afterload relations were derived from these stress-strain relations. Without preload correction, mid wall and endocardial shortening rate were depressed ($p < 0.05$ and $p < 0.005$, respectively) in the hypertrophy group. However, with preload correction at 35 g/cm$^2$, there was no significant difference in shortening rate between the control and hypertrophy groups at afterloads of 150, 200 and 250 g/cm$^2$. Endocardial shortening rate at a preload of 25 versus 35 g/cm$^2$ demonstrated a preload dependence in both the control ($p < 0.04$) and the hypertrophy group ($p < 0.01$). Mid wall shortening rate displayed a preload dependence only in the hypertrophy group ($p < 0.05$).**

**It is concluded that end-systolic stress-strain relations are linear in control conditions and in hypertrophy, fiber shortening rate is preload-dependent and, thus, shortening rate-afterload relations currently used to assess myocardial contractility need to be modified to account for these preload effects.**

***(J Am Coll Cardiol 1990;15:890–9)***

For over two decades, there have been numerous attempts to assess myocardial contractility in both the animal and clinical settings. These attempts have met with moderate success, and for a detailed account of these studies, the reader is referred to the article by Braunwald et al. (1).

The numerous indexes proposed have been based on either the force-velocity concept (2) or the ventricular elastance concept (3). The clinical utility of many of these indexes has been limited because of several factors, including 1) the attempt to develop simple indexes, based on single point measurements, that were later demonstrated to be load dependent; 2) the development of ejection fraction, shortening and shortening rate-afterload relations without preload correction; and 3) the size and load dependence of variables based on the ventricular elastance concept.

The present study addresses several of these issues. In addition, by employing the new concept (4) of systolic myocardial stiffness, it 1) examines the linearity of the end-systolic stress-strain relation in pressure overload hypertrophy induced by banding of the ascending aorta; 2) examines the preload dependence of shortening and shortening rate; and 3) compares this new approach for assessing myocardial contractility with current conventional methods.

## Terminology and Definitions

It is appropriate first to define terms that are employed in the concept of systolic myocardial stiffness (4).

**Stress difference ($\sigma$).** The total stress difference ($\sigma = \sigma_\theta - \sigma_r$) is the difference of the average circumferential ($\sigma_\theta$) and radial ($\sigma_r$) stress components (5,6), assuming that the left

From the Department of Medicine, Brigham and Women's Hospital and Harvard Medical School, Boston, Massachusetts and the New England Regional Primate Research Center, Southborough, Massachusetts. Dr. Fujii's current address is The Children's Hospital, Boston, Massachusetts. This work was supported by Grants HL 34596 and BRSG S07 RR 05950-05 from the National Heart, Lung, and Blood Institute, National Institutes of Health, Bethesda, Maryland.

Manuscript received August 2, 1989; revised manuscript received October 13, 1989, accepted October 26, 1989.

Address for reprints: Israel Mirsky, PhD, Brigham and Women's Hospital, 75 Francis Street, Boston, Massachusetts 02115.



0735-1097/90/$3.50

ventricle may be represented by a cylindrical anulus at the site where the short-axis measurements are made.

**Strain difference ($\varepsilon$).** The associated strain difference ($\varepsilon = e_\theta - e_r$) is the difference of the circumferential ($e_\theta$) and radial ($e_r$) strain components at the *mid wall*. Note that analyses will also be conducted on the basis of *endocardial* strains to compare the results with those of Colan et al. (7).

**Circumferential mid wall natural strain ($\varepsilon_N$).** Natural strain ($\varepsilon_N$) = log(Dm/Dom), where Dm is the instantaneous mid wall minor diameter of the left ventricle and Dom is the minor diameter at zero stress ($\sigma = 0$). The corresponding strain in the endocardium is $\log(D/D_0)$, where D and $D_0$ are, respectively, the instantaneous endocardial and zero stress diameters.

**Average systolic myocardial stiffness (Eav).** $Eav = (3/2)\sigma/\varepsilon = \sigma/(K \times e_\theta)$ where K = 4/3 for a cylindrical geometry and $e_\theta$ = the circumferential strain component at the mid wall (4–6).

**End-systole.** This is the time at which systolic myocardial stiffness attains its maximal value ($Eav_{es}$) and differs from the conventional definition, namely, the time of end-ejection.

## Methods

**Animal preparation.** Pressure overload left ventricular hypertrophy was induced in six mongrel puppies (8 to 10 weeks of age) by banding the ascending aorta distal to the coronary arteries (8,9). The band was implanted through a thoracotomy in the fourth right intercostal space with use of a sterile surgical technique and sodium thiamylal anesthesia (25 mg/kg body weight). The bands were tightened until a thrill could be palpated over the aortic arch. In five puppies designated as sham-operated control puppies, a right thoracotomy was performed, the aortic root was dissected and the chest closed without implantation of a band. Both groups of puppies were allowed to recover from surgery and to grow to maturity, at which time they were instrumented for study.

**Instrument implantation.** These 11 dogs, which have been previously studied (10,11), were instrumented at 12 to 20 months of age through a thoracotomy in the fifth left intercostal space, with use of sterile surgical technique and pentobarbital sodium anesthesia (30 mg/kg intravenously). Tygon catheters (Norton Plastics and Synthetic Company) were implanted in the descending thoracic aorta and apex of the left ventricle. Piezoelectric ultrasonic dimension crystals were implanted on opposing anterior and posterior endocardial surfaces of the left ventricle for measurement of the minor internal diameter and on opposing endocardial and epicardial surfaces for measurement of wall thickness. These latter crystals were implanted in the same equatorial plane as the internal diameter crystals. A solid state pressure transducer (P22, Konigsberg Instruments) was implanted in the apex to measure left ventricular pressure. The thoracotomy incision was closed in layers, and the dogs were allowed to recover for 2 to 4 weeks before study.

The dogs used in this study were maintained in accordance with the guidelines of the Committee on Animals of Harvard Medical School and those prepared by the Committee on Care and Use of Laboratory Animals of the Institute of Laboratory Animal Resources, National Council (DHEW publication No. NIH 78-23, revised 1978).

Statham P23 ID strain gauge manometers (Statham Instruments) were calibrated with a mercury manometer and used to sample aortic and left ventricular pressures from the implanted catheters. Left ventricular pressure was measured using the solid state miniature pressure gauge calibrated in vitro with a mercury manometer and in vivo, employing the left ventricular measurements made with the Statham strain gauge manometers. Left ventricular internal diameter and wall thickness were measured with an ultrasound transit time dimension gauge (12). The dimension gauge generates a voltage linearly proportional to the transit time of the ultrasound impulses traveling at the velocity of $1.58 \times 10^6$ mm/s between the piezoelectric crystals, resulting in a continuous record of left ventricular dimensions. The frequency response of the dimension gauge is flat to 60 Hz. At constant room temperature, the thermal drift of the instrument is minimal (that is, <0.02 mm in 6 h). Any drift in the measurement system was eliminated during the experiment by periodic calibrations accompanied by substituting impulses of known duration from a crystal-controlled pulse generator having a stability of 0.001%. The positions of all transducers were confirmed at autopsy, and positions of the crystals were confirmed in five of the dogs in vivo using fluoroscopic visualization of the heart.

**Experimental protocol.** The data presented have been analyzed for five control dogs and six dogs with left ventricular hypertrophy. Load was altered by the graded infusion of phenylephrine (1, 2, 5 and 10 μg/kg per min). Beta-adrenergic receptor blockade was accomplished by the administration of 2 mg/kg of propranolol to eliminate the sympathetic nervous system-mediated enhancement of contractility in the hypertensive state (11) and the inotropic effect of phenylephrine itself (13).

**Data analysis.** Data were recorded on a multichannel tape recorder (Honeywell 101) and played back on a direct-writing oscillograph (Gould-Brush Mark 200). Continuous records of the first derivative of left ventricular pressure (dP/dt) were derived from the left ventricular pressure signals using Philbrick amplifiers (Teledyne, Philbrick) operated as a differentiator and having a frequency response of 700 Hz. A triangular wave signal was substituted for the pressure signal to calibrate the differentiator directly. Left ventricular end-diastolic dimensions were measured immediately before the onset of ventricular contraction. Left ventricular end-systolic dimensions were measured at the time of the maximal systolic stiffness. The analog signals of

JACC Vol. 15, No. 4
March 15, 1990:890–9

left ventricular pressure, minor diameter and wall thickness were then digitized using an IBM PC/AT computer, with a sampling interval of 2.5 ms. This computer was used to calculate instantaneous left ventricular wall stresses, systolic myocardial stiffness, end-systolic stress-strain relations, shortening-afterload relations and fiber shortening rate-afterload relations.

**Statistics.** Statistical analysis was performed using commercially available software (14), and the data are reported as mean values ± SEM. Unpaired *t* tests were used to determine whether there were differences between the values before and after the induction of left ventricular hypertrophy. Differences were considered significant at $p < 0.05$ (15).

## Theoretic Considerations

curvilinear regression analyses were performed, and tests of significance of departure from linearity (15) were conducted.

3) This iterative procedure was continued until Dom converged to a constant value. If linearity of the stress versus log Dmes relation is established, the linear end systolic stress-strain ($\sigma_{es} - \varepsilon_{es}$) relation may be expressed in the form:

$$\sigma_{es} = \max \text{Eav} \times \varepsilon_{es}, \quad [5]$$

where $\varepsilon_{es} = (4/3) \log(\text{Dmes/Dom})$. Thus, max Eav is the slope of this linear relation and may be used to assess *changes* in myocardial contractility in a given ventricle under certain conditions. Note that two to five beats were analyzed for each intervention.

**Shortening and shortening rate versus afterload relations.** The mid wall shortening-afterload ($S_m - \sigma_{aft}$) relation as

Table 1. Body and Heart Weight (postmortem measurements) in 11 Dogs

| | Control Group (n = 5) | Hypertrophy Group (n = 6) |
|---|---|---|
| Body wt (kg) | 27 ± 1 | 24 ± 2 |
| Left ventricular free wall + septum wt (g) | 121 ± 10 | 176 ± 9* |
| Left ventricular free wall + septum wt/body wt (g/kg) | 4.5 ± 0.2 | 7.6 ± 0.6† |
| Right ventricular wt (g) | 47 ± 3 | 45 ± 4 |
| Right ventricular wt/body wt (g/kg) | 1.8 ± 0.1 | 1.9 ± 0.1 |

*$p < 0.005$, †$p < 0.001$ (different from control). Values are mean ± standard error of the mean. wt = weight.

**Baseline data (Table 2).** Left ventricular pressure in the dogs with hypertrophy was significantly higher ($p < 0.001$) than in the control group (180 ± 5 versus 135 ± 5 mm Hg, respectively); however, the end-diastolic pressure was similar (10 ± 2 versus 9 ± 2 mm Hg, respectively). End-diastolic and end-systolic diameters for both groups were similar, but wall thickness differed significantly, being 40% greater in the hypertrophy group. Although there was a significant difference ($p < 0.01$) in *mid wall* circumferential shortening rate (Vcfm) (0.50 ± 0.04 control versus 0.32 ± 0.03 $s^{-1/2}$ hypertrophy), endocardial shortening rate (Vcfe) was similar in both groups. End-systolic stress was not significantly different, but integrated mean stress during ejection was significantly lower ($p < 0.05$) in the hypertrophy group (197 ± 6 control versus 149 ± 17 $g/cm^2$ hypertrophy).

**Linearity of the end-systolic stress-strain relations.** Figure 1 displays the end-systolic stress difference versus log diameter relations ($\sigma_{cs}$ versus log Dmes) for typical experiments in the control (Fig. 1A) and hypertrophy groups (Fig. 1B). F tests (15) indicated no departure from linearity. Extrapolation of these relations yielded the mid wall diameter at zero stress (Dom) and the associated end-systolic stress-strain relations (Fig. 1C). In all cases (five control, six left ventricular hypertrophy), F tests demonstrated no significant departure from linearity.

**Slope of the end-systolic stress-strain relation and diameter at zero stress.** Based on a mid wall analysis, the slopes (max Eav) and diameters (Dom) were similar in the two groups (2,150 ± 246 hypertrophy versus 2,913 ± 494 $g/cm^2$ control) and (45.7 ± 1.4 hypertrophy versus 42.5 ± 1.2 mm control). In contrast, the endocardial analysis indicated that the slope (Max Eav) was markedly depressed ($p < 0.03$) in the hypertrophy group (829 ± 138 hypertrophy versus 1,362 ± 159 $g/cm^2$ control); however, diameters (Do) were similar (22.0 ± 1.8 hypertrophy versus 26.1 ± 1.0 mm control).

**Mid wall shortening rate-afterload relations.** Figure 2A displays a plot of the preload uncorrected shortening rate-afterload points (Vcfm − $\sigma_{aft}$) with the associated 95% confidence bands for the entire control group. These points were obtained in the control state and at graded doses of 1, 2, 5 and 10 μg/kg per min of phenylephrine.

Employing equations 6 and 7, the control shortening rate-afterload relation corrected for preload ($\sigma_{ed}$ = 35 $g/cm^2$) is displayed in Figure 2B. The individual shortening rate-

Table 2. Baseline Left Ventricular Hemodynamic, Function and Dimension Variables in 11 Dogs

| | Control Group (n = 5) | Hypertrophy Group (n = 6) |
|---|---|---|
| End-diastolic pressure (mm Hg) | 9 ± 2 | 10 ± 2 |
| End-systolic pressure (mm Hg) | 125 ± 5 | 160 ± 7* |
| Peak systolic pressure (mm Hg) | 135 ± 5 | 180 ± 5† |
| Maximal first derivative of pressure (mm Hg/s) | 2,959 ± 329 | 2,839 ± 197 |
| End-diastolic endocardial diameter (mm) | 38.9 ± 0.9 | 33.7 ± 2.1 |
| End-systolic endocardial diameter (mm) | 29.8 ± 0.9 | 26.6 ± 2.0 |
| End-diastolic mid wall diameter (mm) | 52.1 ± 0.8 | 53.2 ± 2.0 |
| End-systolic mid wall diameter (mm) | 45.4 ± 1.0 | 49.0 ± 1.5 |
| End-diastolic wall thickness (mm) | 13.2 ± 0.5 | 19.5 ± 1.2‡ |
| End-systolic wall thickness (mm) | 15.6 ± 0.7 | 22.4 ± 1.4‡ |
| Endocardial shortening fraction (%) | 23.5 ± 1.3 | 21.5 ± 2.7 |
| Mid wall circumferential shortening fraction (%) | 12.9 ± 0.9 | 7.9 ± 0.8‡ |
| Radial wall thickening fraction (%) | 18.6 ± 2.7 | 15.2 ± 2.5 |
| Shortening time (ms) | 201 ± 7 | 168 ± 7* |
| Heart rate (beats/min) | 100 ± 6 | 128 ± 4‡ |
| Endocardial shortening rate ($s^{-1/2}$) | 0.91 ± 0.05 | 0.87 ± 0.09 |
| Mid wall circumferential shortening rate ($s^{-1/2}$) | 0.50 ± 0.04 | 0.32 ± 0.03* |
| Average end-diastolic stress ($g/cm^2$) | 18 ± 3 | 12 ± 2 |
| Average end-systolic stress ($g/cm^2$) | 162 ± 8 | 137 ± 20 |

*$p < 0.01$, †$p < 0.001$, ‡$p < 0.005$ (different from control). Values are mean ± standard error of the mean.

JACC Vol. 15, No. 4
March 15, 1990:896–9

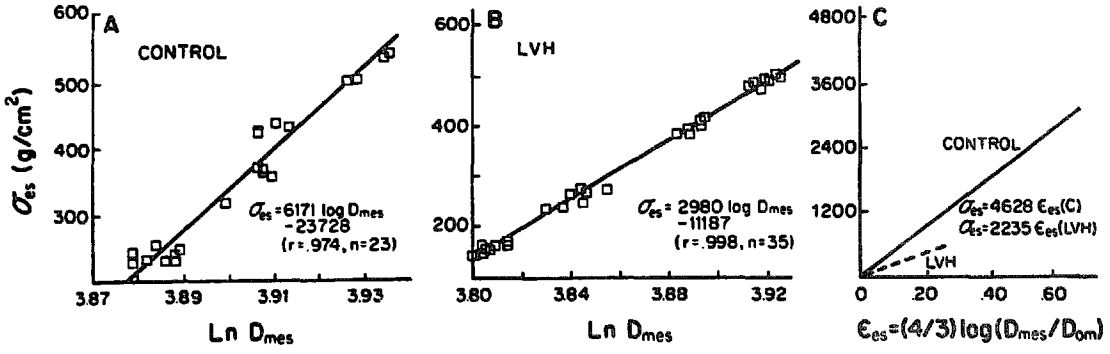


**Figure 1.** End-systolic stress difference ($\sigma_{es}$) versus log minor diameter at end-systole (Dmes) relations in control (A) and left ventricular hypertrophy (LVH) (B) groups and associated stress-strain relations (C). Afterload was altered by graded doses of phenylephrine (1, 2, 5, and 10 μg/kg per min). F tests indicated no departure from linearity (Ln), and linear extrapolation yielded the mid wall diameter ($D_{om}$) at zero stress. The end-systolic stress-strain relations (C) were obtained directly from the relations in panels A and B, employing $D_{om}$ as the reference length.

afterload relations for the hypertrophy group uncorrected and corrected for preload are shown in Figures 2C and 2D, respectively.

Comparisons of shortening rate between the control and hypertrophy groups at common afterload levels of 150, 200 and 250 g/cm$^2$ and uncorrected for preload (conventional method) are exhibited in Figure 3A. In this analysis, the shortening rate at each afterload level was calculated from a linear regression of the raw data points for each dog. At each level of afterload, shortening rate was significantly depressed ($p < 0.005$) in the hypertrophy group. Figures 3B and C show the corresponding comparisons at two different levels of preload ($\sigma_{ed}$ = 25 and 35 g/cm$^2$). Equations 6 and 7 were used in this analysis and values for minor diameters at end-diastole (Dmed) at given preloads were obtained from curve fits of the end-diastolic stress-diameter relations ($\sigma_{ed}$ versus Dmed). At a preload level of 25 g/cm$^2$ (Fig. 3B), there was a borderline significant difference ($p < 0.05$) in shortening rate between the two groups; however, at preload $\sigma_{ed}$ = 35 g/cm$^2$, there was no significant difference between control and hypertrophy groups at each afterload level.

**Preload dependence of shortening rate.** A paired *t* test for mid wall shortening rate at preloads 25 and 35 g/cm$^2$ was conducted at each level of afterload and indicated a preload dependence in the hypertrophy group only ($p < 0.05$). In contrast, endocardial shortening rate demonstrated a preload dependence in both control ($p < 0.04$) and hypertrophy ($p < 0.01$) groups.

**End-systolic pressure-diameter relation.** Employing with use of an F test (15), departure from linearity of the end-systolic pressure-diameter relation was observed in five of six dogs in the hypertrophy group and in only two of five dogs in the control group (Fig. 4).

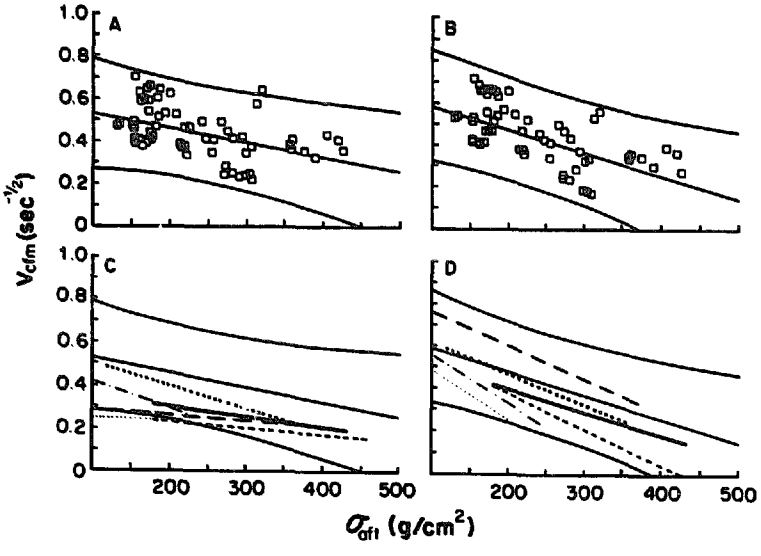


**Figure 2.** Mid wall shortening rate-afterload relations. A, Shortening rate-afterload relation (preload uncorrected) and associated 95% confidence bands for the five dogs in the control group. B, Preload-corrected ($\sigma_{ed}$ = 35 g/cm$^2$) shortening-afterload relation and associated 95% confidence bands for the entire control group. C and D, Individual shortening rate-afterload relations uncorrected (C) and corrected for preload (D) for the six dogs with left ventricular hypertrophy. Note the qualitative differences in the assessment of myocardial contractility as obtained by the conventional method (C) and the present approach (D). Vcfm = mid wall circumferential fiber shortening rate; $\sigma_{aft}$ = end-systolic circumferential stress = afterload.

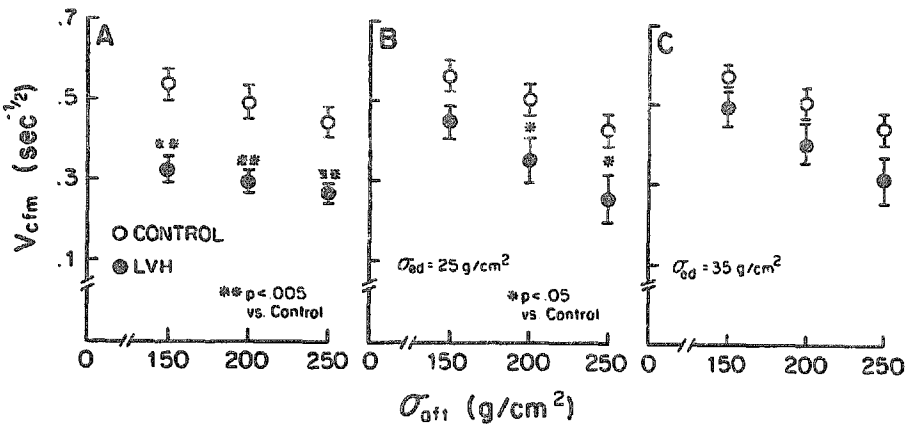


Figure 3. Comparisons of contractile state between the control and hypertrophy groups at various levels of afterload. Without preload correction, the conventional method (A) clearly indicates a depression of the contractile state in the left ventricular hypertrophy (LVH) group. In contrast, the preload-corrected relations indicate a borderline significant difference at 25 g/cm$^2$ and no significant difference at preload ($\sigma_{ed}$) = 35 g/cm$^2$. Other abbreviations as in Figure 2.

## Discussion

**Assessment of myocardial contractility.** The mean fiber shortening rate-afterload relation (16) has been widely used in experimental and clinical settings to assess myocardial contractility because it has been assumed to be independent of preload (17–19). However, in all these and other studies (16–19), preload and afterload were allowed to vary simultaneously, endocardial shortening rate was evaluated, and single point measurements obtained from individual animals or patients were used to construct the shortening rate-afterload relation. In some cases, afterload was varied slightly (18) or it was not evaluated (19). The exception to these studies was the unique study by Colan et al. (7), in which preload was augmented individually in a number of pediatric patients and shortening rate-afterload relations subsequently were constructed. Although they concluded that shortening rate was independent of preload, their studies were noninvasive; hence, preload (end-diastolic stress) could not be evaluated, and afterload (end-systolic stress) calculations were based on several simplifying assumptions. It is, therefore, conceivable that the counterbalancing effects of preload and afterload on shortening rate could have yielded a result demonstrating preload independence. Another possible explanation is that mid wall and endocardial shortening rates may yield contrasting results, and these points will be discussed later.

Figure 4. End-systolic pressure-diameter relations in control (C) and left ventricular hypertrophy (LVH) groups. Generally, these relations were nonlinear in the hypertrophy group (five of six dogs) and linear in the control group (three of five dogs). Thus, the employment of slope changes of these relations to assess changes in ventricular contractility must be considered with caution. Des = diameter at end-systole; PE = phenylephrine (in μg/kg per min); Pes = pressure at end-systole.

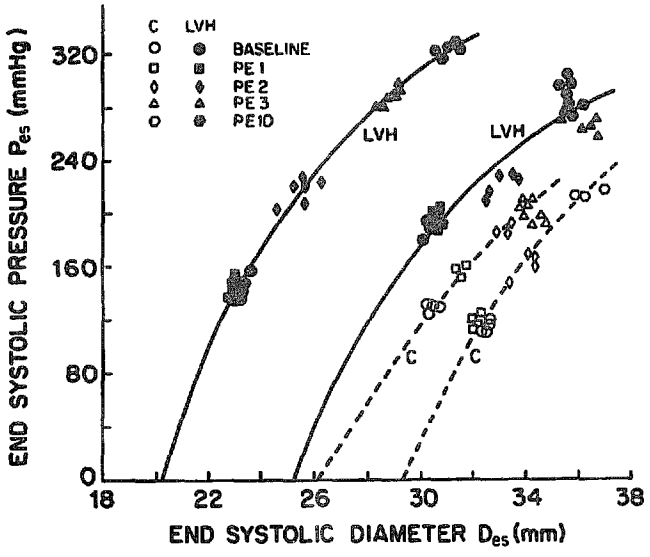


**Linearity of the end-systolic stress-strain relation.** Earlier studies (4) demonstrated linearity of the end-systolic stress-strain relations in control conscious dogs, and the present study has established that this is also the case in dogs with moderate left ventricular hypertrophy induced by aortic banding. The linearity of this relation has important clinical implications because it implies that the slope (max Eav) is independent of load. Thus, if the ventricle is used as its own control, changes in this slope after a given intervention reflect changes in the inotropic state provided the diameter at zero stress (Dom) is not significantly altered. This result is apparent from equation 6 for mid wall shortening (Sm), where it is observed that changes in max Eav result in changes in Sm if Dom, "preload"(Dmed) and afterload ($\sigma_{aft}$) are maintained constant. It must be emphasized, however, that max Eav does not assess myocardial contractility, but represents systolic or active myocardial stiffness and may alternatively be termed myocardial elastance. This is evident from the clinical studies (20) that show that the slope of end-systolic stress-strain relations (max Eav) is markedly elevated in patients with aortic stenosis with moderate left ventricular hypertrophy in the presence of normal myocardial function in contrast to patients with severe mitral regurgitation who have near normal values of max Eav but depressed myocardial function as assessed by the preload-corrected ejection fraction-afterload relation. Similar state-

JACC Vol. 15, No. 4
March 15, 1990:890–9

ments can be made with regard to Emax and $E_{es}$ (slopes of the end systolic pressure-volume relation in the ventricular elastance concept [3]), namely, that they represent systolic chamber stiffness variables and not ventricular contractility variables (21,22).

**Mid wall versus endocardial shortening rate and shortening.** At the outset, a distinction has to be made between circumferential mid wall shortening rate (Vcfm) and endocardial shortening rate (Vcfe). In the mid wall region, the fibers are oriented predominantly in the circumferential direction and, therefore, shortening takes place mainly in this direction. In contrast, shortening at the endocardium (where fibers are primarily oriented parallel to the endocardial surface) is mainly by radial wall thickening of fibers in the subendocardial layers, as noted by several investigators (23–25). In fact, Calderon et al. (26) postulated that because ejection fraction results from shortening in longitudinal, circumferential and radial directions, it may have a different interpretation in pressure overload hypertrophy relative to volume overload hypertrophy. It is, therefore, not surprising in view of these studies (23–26) to observe conflicting results (Table 2) that indicate no significant differences in baseline endocardial shortening and shortening rate between control and hypertrophy groups in contrast to depressed mid wall shortening and mid wall shortening rate in the hypertrophy group. Furthermore, because left ventricular wall stress (as distinct from fiber stress) is higher at the endocardium than at the mid wall (27), one might incorrectly conclude that a hypercontractile state exists in the subendocardial layers. Thus, considerable caution must be exercised in the interpretation of many published studies relating to endocardial shortening and shortening rate.

**Comparison of shortening rate versus afterload analyses based on present and conventional methods.** In the present study and most other studies, preload and afterload were allowed to vary simultaneously; thus, the measurements of shortening rate are the result of two counterbalancing effects. Figure 5 displays the method for developing the shortening rate-afterload relations in four dogs with left ventricular hypertrophy. In the conventional method (7), the shortening rate-afterload relation (dotted line) is obtained by the linear regression of points that lie on contractile state relations with different preload levels, whereas in the current method, these relations are developed for each preload level. Thus, the preload dependence of shortening rate is readily observed.

Figure 6, which displays the afterload versus preload relations for both control and hypertrophy groups, provides indirect evidence as to why the conventional method yields a result indicating an apparent depression of the contractile state in the hypertrophy group. Note that for any given afterload, preload is much lower in the hypertrophy group than in the control group. This has the effect, therefore, of lowering the shortening rate in hypertrophy at each level of

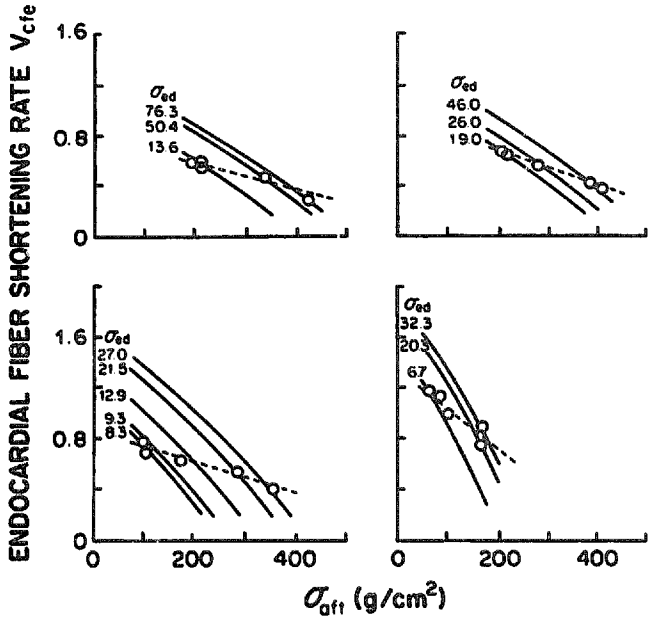


**Figure 5.** Development of the endocardial shortening rate-afterload relations in four dogs with left ventricular hypertrophy based on conventional and present methods. In each case, the dotted line represents the linear regression of points that lie on contractile state relations at different preload levels (conventional method). This contrasts with the present method where the relations are developed for each prescribed preload level ($\sigma_{ed}$) and clearly display the preload dependence of shortening rate, a result in disagreement with studies by Colan et al. (7). Open circles represent average values obtained from two to five beats for each drug intervention. Vcfe = endocardial fiber shortening rate, which was used in the previous studies (7). Other abbreviations as in Figure 2.

afterload, thus artifactually resulting in a depression of contractility. When preload is accounted for, the results generally indicate that myocardial function remains within normal limits in hypertrophy. Note, however, that at a preload of 25 g/cm$^2$, the results based on mid wall shortening rate indicated depressed myocardial function in hypertrophy (Fig. 3B). On closer examination, it was revealed that in one of the dogs with hypertrophy, shortening rate was either unusually small or negative for afterloads > 200 g/cm$^2$. Omission of these data from the statistical analysis resulted in normal myocardial function in the hypertrophy group.

Most animal and clinical studies relating to myocardial contractility in hypertrophy report only mean values of these variables for control and hypertrophy groups, and generally there are disagreements among the various studies. These differences may be due not only to the different methodologies employed, but also to heterogeneity of the patients or animals studied. In our study, the left ventricular hypertrophy induced in each dog also varied; however, the advantage of the present method is the ability to assess the shortening rate-afterload relation for each individual dog at a prescribed preload. Figures 2C and D, which display these individual

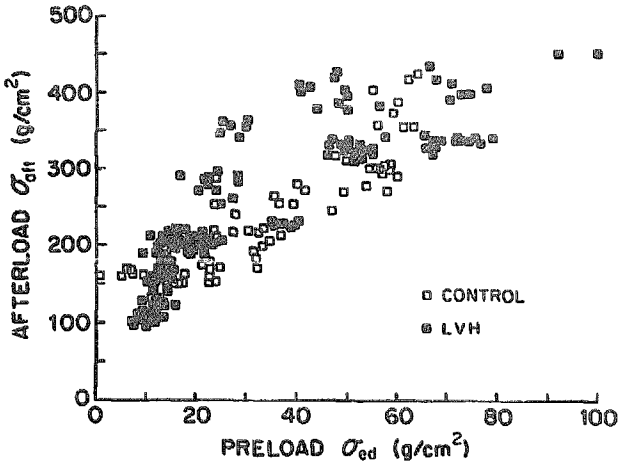


**Figure 6.** Afterload versus preload relations for control and left ventricular hypertrophy (LVH) groups. Note that at a given level of afterload, preload generally is much lower in hypertrophy than in the control group, resulting in an artifactual depression of contractility in hypertrophy when preload is not accounted for. It is also interesting to observe that preload becomes negative when afterload is zero. Abbreviations as in Figure 2.

relations for the hypertrophy group without and with preload correction, clearly show marked qualitative differences, thus emphasizing the importance of preload correction.

**End-systolic pressure-diameter relation.** The slope of the end-systolic pressure-diameter relation has been employed as an index of ventricular contractility by a number of investigators. Because the slope is size dependent (by definition) and the assumption of linearity is not always validated, the utility of this index is limited.

It is apparent from the present study that the theoretic pressure-diameter relation (equation 9) is nonlinear, and although linearity could be observed in three of five control dogs, this occurred in only one of six dogs in the hypertrophy group. However, linearity of the end-systolic pressure-diameter relation does not necessarily imply linearity of the end-systolic pressure-volume relation. Thus, at best, changes in slope of the pressure-diameter relation in a given ventricle may reflect changes in ventricular contractility in some situations where the zero stress diameter (Dom) remains unaltered after an intervention.

**Limitations of the analysis.** There are several limitations to the present study. These include: 1) estimations of zero stress diameters (Dom and Do) based on linear extrapolations of stress versus log (diameter) relations (Fig. 1). Because measurements of pressure and diameter were not made at very low afterloads, the possibility remains that end-systolic stress-strain relations may be nonlinear, as observed by Takeda et al. (28). In this regard, it might be possible to predict the behavior of the stress-strain relations in the low stress range by examining in more detail the afterload versus preload relations (Fig. 6) and end-systolic versus end-diastolic pressure relations. For example, when afterload is zero, preload becomes negative and, thus, one could obtain estimates of the pressures when zero-developed pressure occurs (that is, occurrence of a "dead" volume [29]). 2) The assumption of a cylindrical model needs further validation, and this could be evaluated by the inclusion of long-axis measurements in future studies. 3) The importance of ventricular/vascular coupling also requires additional study in a manner similar to that conducted by Latham et al. (30).

**Conclusions.** The present investigation demonstrates: 1) linearity of the end-systolic stress-strain relations in moderate left ventricular hypertrophy, thus permitting the development of preload-corrected shortening/shortening rate-afterload relations that are used to assess myocardial contractility for a given preload. 2) Shortening rate is preload-dependent and, therefore, preload corrections are necessary for a more reliable assessment of myocardial contractility. In this regard, mid wall shortening/shortening rate should be employed in preference to endocardial shortening/shortening rate, which is contributed to mainly by radial wall thickening of the subendocardial layers. 3) Finally, end-systolic pressure-diameter relations are generally nonlinear in left ventricular hypertrophy; thus, caution must be exercised when associating slope changes in these relations with changes in ventricular contractility.

# Appendix

*1. Expressions for Average Stress Difference, Preload and Afterload*

It is assumed that the left ventricle may be represented by a cylindrical anulus at the site where the short-axis measurements are made. Thus, at any given radius (r), the circumferential ($\sigma_\theta$) and radial ($\sigma_r$) stress components in this anulus are given by (31):

$$\sigma_\theta = 1.36 \times P \times a^2 (1 + b^2/r^2)/(b^2 - a^2)$$

$$\sigma_r = 1.36 \times P \times a^2 (1 - b^2/r^2)/(b^2 - a^2). \quad [1.1]$$

where P is the left ventricular cavity pressure and a and b are, respectively, the inner and outer radius. Note that a = D/2 and b = D/2 + h, where D is the endocardial short axis diameter and h is the left ventricular wall thickness.

*The integrated mean circumferential and radial stresses are, therefore, expressed as:*

$$\sigma_{\theta c} = \int_a^b \sigma_\theta \, dr/(b - a) = 1.36 \times (PD/2h)$$

$$\sigma_{rc} = \int_a^b \sigma_r \, dr/(b - a) = -1.36 \times PD/2(D + h). \quad [1.2]$$

Hence, the stress difference is

$$\sigma = \sigma_{\theta c} - \sigma_{rc} = 1.36 \times (PD/2h)[1 + h/(D + h)]$$

$$= \sigma_{\theta c} (1 + h/(D + h)). \quad [1.3]$$

JACC Vol. 15, No. 4
March 15, 1990:890–9

*Preload and afterload are respectively defined as:*

$$\sigma_{ed} = (\sigma_{\theta c})_{ed} = 1.36 \times (PD/2h)_{ed}$$

$$\sigma_{aft} = (\sigma_{\theta c})_{es} = 1.36 \times (PD/2h)_{es}, \quad [1.4]$$

where ed and es refer to end-diastole and end-systole, respectively.

*2. Shortening-Afterload Relation*

The expressions used to determine the mid wall shortening-afterload relation (Sm – $\sigma_{aft}$) are:

$$\sigma_{es} = (4/3) \text{ max Eav} \times \log (Dm_{es}/Dom) \quad [2.1]$$

$$Sm = (Dm_{ed} - Dm_{es})/Dm_{ed} \quad [2.2]$$

$$\sigma_{es} = \alpha + \beta\ \sigma_{aft}, \quad [2.3]$$

where $\alpha$ and $\beta$ are constants obtained by linear regression, and all other quantities have been previously defined. Elimination of Dmes and $\sigma_{es}$ from the above expressions yields the relation between shortening and afterload, namely:

$$Sm = 1 - Dmes/Dmed$$

$$= 1 - (Dom/Dmed) \times \exp [\sigma_{es}/(4/3) \text{ max Eav}]$$

$$= 1 - (Dom/Dmed) \times \exp [(\alpha + \beta\ \sigma_{aft})/(4/3) \text{ max Eav}]. \quad [2.4]$$

It should be noted that equation 2.3 between $\sigma_{es}$ and $\sigma_{aft}$ is linear over the measured range of data only, and becomes nonlinear at low values of $\sigma_{es}$ and $\sigma_{aft}$.

*3. End-Systolic Pressure-Endocardial Diameter Relation*

From the end-systolic stress-endocardial strain relation (similar to equation 5 in the text), one obtains:

$$\sigma_{es} = \text{max Eav} \times \epsilon_{ese} = (4/3) \text{ max Eav} \times \log (Des/Do), \quad [3.1]$$

where max Eav is the slope of the linear end-systolic stress-endocardial strain relation and $\epsilon_{ese}$ = (4/3) log (Des/Do) is the endocardial strain difference at end-systole. By curve-fitting the ratio ($\sigma_{es}/P_{es}$) in the form:

$$\sigma_{es}/P_{es} = \gamma + \delta\ Des,$$

we obtain

$$P_{es} = \sigma_{es}/(\gamma + \delta\ Des) \quad [3.2]$$

$$= [(4/3) \text{ max Eav}/(\gamma + \delta\ Des)] \times \log (Des/Do).$$

We are indebted to S. F. Vatner, MD for permitting these studies to be conducted in his laboratory at the New England Primate Research Center in Southborough, Massachusetts.

## References

1. Braunwald E, Sonnenblick EH, Ross J Jr. Contraction of the normal heart. In: Braunwald E. Heart Disease. vol. 1, Philadelphia: WB Saunders, 1984:409–46.
2. Sonnenblick EH. Force-velocity relations in mammalian heart muscle. Am J Physiol 1962;202:931–9.
3. Suga H, Sagawa K. Instantaneous pressure-volume relationships and their role in the excised supported canine left ventricle. Circ Res 1974;35:117–26.
4. Mirsky I, Tajimi T, Peterson KL. The development of the entire end-systolic pressure-volume and ejection fraction-afterload relations: a new concept of systolic myocardial stiffness. Circulation 1987;76:343–56.
5. Mirsky I, Rankin JS. The effects of geometry, elasticity and external pressure on the diastolic pressure-volume and stiffness-stress relations: how important is the pericardium? Circ Res 1979;44:601–11.
6. Aoyagi T, Fujii AM, Gelpi RJ, Hittinger L, Crocker VM, Mirsky I. Application of the systolic stiffness concept to assess myocardial function in developing hypertension. Jpn Heart J (in press).
7. Colan SD, Borow KM, Neumann A. Left ventricular end-systolic wall stress-velocity of fiber shortening relation: a load-independent index of myocardial contractility. J Am Coll Cardiol 1984;4:715–24.
8. Kleinman LH, Wechsler AS, Rembert JC, Fedor JM, Greenfield JC. A reproducible model of moderate to severe concentric left ventricular hypertrophy. Am J Physiol 1978;234:H515–24.
9. O'Kane HO, Geha AS, Kleiger RE, Abe T, Salaymeh MT, Malik AB. Stable left ventricular hypertrophy in the dog. J Thorac Cardiovasc Surg 1973;65:264–71.
10. Fujii AM, Vatner SF, Serur J, Als A, Mirsky I. Mechanical and inotropic reserve in conscious dogs with left ventricular hypertrophy. Am J Physiol 1986;251:H815–23.
11. Gelpi RJ, Hittinger L, Fujii AM, Crocker VM, Mirsky I, Vatner SF. Sympathetic augmentation of cardiac function in developing hypertension in conscious dogs. Am J Physiol 1988;255:H1525–34.
12. Pagani M, Baig H, Sherman A, et al. Measurement of multiple simultaneous small dimensions and study of arterial pressure-dimension relations in conscious animals. Am J Physiol 1978;235:H610–7.
13. Tajimi T, Widman TF, Matsuzaki M, Peterson KL. Differing effect of angiotensin II and phenylephrine on end-systolic pressure-volume relationship in conscious dogs (abstr). J Am Coll Cardiol 1984;3:523.
14. Marijia J. Statistical Package for the Social Sciences. Chicago: SPSS Inc., 1988.
15. Snedecor GW, Cochran WF. Statistical Methods, ed. 6. Ames, IA: Iowa State University Press, 1967:549,453.
16. Karliner JS, Gault JH, Eckberg D, Mullins CB, Ross J Jr. Mean velocity of fiber shortening: a simplified measure of left ventricular myocardial contractility. Circulation 1971;44:323–33.
17. Mahler F, Ross J Jr, O'Rourke RA, Covell JW. Effects of changes in preload, afterload and inotropic state on ejection and isovolumic phase measures of contractility in the conscious dog. Am J Cardiol 1975;35:624–34.
18. Quinones MA, Gaasch WH, Alexander JK. Influence of acute changes in preload, afterload, contractile state and heart rate on ejection and isovolumic indices of myocardial contractility in man. Circulation 1976; 53:293–302.
19. Nixon JV, Murray RG, Leonard PD, Mitchell JH, Blomqvist. Effect of large variations in preload on left ventricular performance characteristics in normal subjects. Circulation 1982;65:698–703.
20. Mirsky I, Corin WJ, Murakami T, Grimm J, Hess OM, Krayenbuehl HP. Correction for preload in assessment of myocardial contractility in aortic and mitral valve disease: application of the concept of systolic myocardial stiffness. Circulation 1988;78:68–80.

21. Kass DA, Maughan WL. From "Emax" to pressure-volume relations: a broader view. Circulation 1988;77:1203–12.

22. Mirsky I. An appraisal of ventricular and myocardial function variables based on the elastance concept (editorial comment). J Am Coll Cardiol 1989;14:354–6.

23. Gould KL, Kennedy JW, Frimer M, Pollack GH, Dodge HT. Analysis of wall dynamics and directional components of left ventricular contraction in man. Am J Cardiol 1976;38:322–31.

24. Sabbah HN, Marzilli M, Stein PD. The relative role of subendocardium and subepicardium in left ventricular mechanics. Am J Physiol 1981;240: H920–6.

25. Gallagher KP, Matsuzaki M, Osakada G, Kemper WS, Ross J Jr. Effect of exercise on the relationship between myocardial blood flow and systolic wall thickening in dogs with acute coronary stenosis. Circ Res 1983;52:716–29.

26. Calderon J, López-Sendón J, Almeida P. Significance of ejection fraction in hypertrophy and dilatation (abstr). Eur Heart J 1981;2(suppl A):81.

27. Mirsky I. Left ventricular stresses in the intact human heart. Biophys J 1969;9:189–208.

28. Takeda K, Sunnizu T, Yamamoto H, Yagi S. Human left ventricular end-systolic pressure-volume relationship in a cylinder model. Jpn Heart J 1988;29:689–707.

29. Sagawa K. The end-systolic pressure-volume relation of the ventricle: definition, modifications, and clinical use (editorial). Circulation 1981;63: 1223–7.

30. Latham RD, Rubal BJ, Sipkema P, et al. Ventricular/vascular coupling and regional arterial dynamics in the chronically hypertensive baboon: correction with cardiovascular structural adaptation. Circ Res 1988;63: 798–811.

31. Timoshenko S, Goodier JN. Theory of Elasticity. 2nd ed. New York: McGraw-Hill, 1951:59–60.